



Published in final edited form as:

Biomaterials. 2017 June ; 129: 139–151. doi:10.1016/j.biomaterials.2017.03.018.

Mitigating Hypoxic Stress on Pancreatic Islets via *In situ* Oxygen Generating Biomaterial

Maria M. Coronel^{1,2,3}, Ryan Geusz⁴, and Cherie L. Stabler^{1,2,3,4,*}

¹Department of Biomedical Engineering, University of Florida, Gainesville, FL, USA

²Diabetes Research Institute, University of Miami, Miami, FL, USA

³Department of Biomedical Engineering, University of Miami, Miami, FL, USA

⁴Department of Biochemistry and Molecular Biology, University of Miami, Miami, FL, USA

Abstract

A major obstacle in the survival and efficacy of tissue engineered transplants is inadequate oxygenation, whereby unresponsive oxygen tensions result in significant cellular dysfunction and death within the implant. In a previous report, we developed an innovative oxygen generating biomaterial, termed OxySite, to provide supportive *in situ* oxygenation to cells and prevent hypoxia-induced damage. Herein, we explored the capacity of this biomaterial to mitigate hypoxic stress in both rat and nonhuman primate pancreatic islets by decreasing cell death, supporting metabolic activity, sustaining aerobic metabolism, preserving glucose responsiveness, and decreasing the generation of inflammatory cytokines. Further, the impact of supplemental oxygenation on *in vivo* cell function was explored by the transplantation of islets previously co-cultured with OxySite into a diabetic rat model. Transplant outcomes revealed significant improvement in graft efficacy for OxySite-treated islets, when transplanted within an extrahepatic site. These results demonstrate the potency of the OxySite material to mitigate activation of detrimental hypoxia-induced pathways in islets during culture and highlights the importance of *in situ* oxygenation on resulting islet transplant outcomes.

Keywords

Hypoxia; Oxygen; Beta-cell stress; Biomaterials

*Corresponding author: Professor Cherie L. Stabler, Department of Biomedical Engineering, University of Florida, 1275 Center Drive, Gainesville, FL 32611, cstabler@bme.ufl.edu, Telephone: 352-273-9327.

Publisher's Disclaimer: This is a PDF file of an unedited manuscript that has been accepted for publication. As a service to our customers we are providing this early version of the manuscript. The manuscript will undergo copyediting, typesetting, and review of the resulting proof before it is published in its final citable form. Please note that during the production process errors may be discovered which could affect the content, and all legal disclaimers that apply to the journal pertain.

Disclosure statement. C.L.S. holds a patent on the OxySite material.

Author contributions. M.M.C. and C.L.S. developed the concept. M.M.C. and C.L.S. designed the study and analyzed data. M.M.C. conducted all experiments and collected data. R.G. assisted in mRNA expression experiments. M.M.C. and C.L.S. analyzed data and wrote the manuscript.

1. Introduction

Clinical islet transplantation provides an attractive approach to restore endogenous insulin control for Type 1 Diabetics [1, 2]. Poor islet engraftment following transplantation, however, significantly hampers long-term islet function; leading to the need for multiple transplants to achieve glycemic control [1, 3]. While numerous factors contribute to poor islet survival, hypoxia, both in culture and during engraftment, has been identified as a major contributor [4–7]. Hypoxic islets exhibit stabilization of hypoxia-inducible factor-1 α (HIF-1 α), which results in the activation of multiple deleterious responses, including the loss of glucose-stimulated-insulin-secretion, elevated apoptosis, activation of caspase cascades, release of inflammatory cytokines, and defragmentation of islet structure [8, 9]. This HIF-1 α mediated cascade is activated from the start of islet procurement, as islets suffer from fluctuations in ambient oxygen tension during pancreas processing due to the stripping of their native vasculature. Cultured islet spheroids continue to experience unfavorable oxygen gradients, despite the practice of low cell density culture [10, 11]. These detrimental oxygen conditions are intensified following intrahepatic transplantation, as grafts become hypoxic due to inadequate site oxygenation [12, 13]. The significant delay in islet revascularization and the inadequate resulting vascular network results in continuation of these unfavorable oxygen gradients [14]. Thus, interventions focused on improving islet oxygenation during culture and in the early engraftment period could be highly beneficial.

We have previously reported the development of a biomaterial capable of *in situ* oxygen generation, herein termed OxySite [15]. The degree of oxygen supplementation provided by OxySite can be modulated via biomaterial design parameters (e.g. reactive product loading and geometry) to tailor oxygen tensions to the needs of the cultured islets. In this study, we sought to evaluate the impact of oxygen supplementation using OxySite on *in vitro* culture conditions that mimic the common transplant environment (e.g. physiologically relevant oxygen tensions and high loading densities). Of particular emphasis was elucidating the effects of OxySite on islet viability, glycolysis, inflammatory cytokines, and angiogenesis. Establishing the benefits of OxySite supplementation serves the dual purpose of demonstrating its appeal in improving current pancreatic islets culture systems in a cost effective manner, as well as revealing the potential of this material to improve islet engraftment and function *in vivo*.

2. Research Design and Methods

2.1 OxySite Fabrication

OxySite was fabricated as previously described, but with modifications to improve the consistency of CaO₂ distribution and casting [15]. Briefly, 25% w/w CaO₂ (Sigma Aldrich, purity > 70%) was added to PDMS (NUSIL 6215, clinical-grade, mixed 4:1 v/v with catalyst) and mixed/defoamed (Thinky Mixer). The mixture was poured into a cylindrical mold (100 mm; 1 mm thickness) and cured overnight (40 °C). Prior to use, 10 mm OxySite disks were punched out and sterilized with ethanol (30 min). Based on dimensional analysis, it was estimated that 111 mg of CaO₂ was entrapped in each disk. The capacity of OxySite to impart changes in pH and/or H₂O₂ concentrations was tested by placing either a control PDMS or OxySite disk (n =3 per time point) in CMRL cultures (1 mL) in 24-well plates at

37 °C for 5 days. Culture media pH (sensor probe, Miller Toledo) was measured daily. Samples for hydrogen peroxide were collected, with fully refreshment of media, at 24 hr for day 1 and every 48 hrs thereafter until day 5. Hydrogen peroxide concentration was measured using a colorimetric assay (Assay Designs).

2.2 Islet Isolation and Culture

All animal procedures were performed under protocols approved by the University of Miami or University of Florida IACUC and in accordance with National Institutes of Health guidelines. Rat islet isolations were performed using male Lewis rats (Envigo), as described previously [16]. Nonhuman primate (NHP) islets, isolated from Cynomolgus monkeys, were donated from Dr. Norma Kenyon's laboratory (Diabetes Research Institute, University of Miami) [17]. Rat and NHP islets were cultured as previously described prior to experimentation [16].

2.3 Multiphysics Modeling

COMSOL Multiphysics 5.2a was used to implement finite element analysis of oxygen gradients within 2-D islet cultures at different loading densities and oxygen tensions. Models employed followed methods published in Buchwald et al [18]. Briefly, the general diffusion equation with negligible convection was implemented to model oxygen diffusion.

$$\frac{\partial c}{\partial t} + \nabla \cdot (-D\nabla c) = R \quad (1)$$

The reaction rate term for oxygen consumption was modeled as a Michaelis-Menten reaction (2),

$$R_{O_2} = R_{Max,O_2} \frac{C_{O_2}}{C_{O_2} + C_{MM,O_2}} \cdot \delta(C_{O_2} > C_{cr}) \quad (2)$$

with C_{O_2} representing the oxygen concentration within the islet subdomain and the constant term, C_{MM} , corresponding to a critical oxygen level where cellular oxygen consumption decreases by 50% (e.g. C_{MM} equal to $1e-3$ mol/m³) [19]. A maximum oxygen consumption rate R_{max} of 0.034 mol·s⁻¹·m⁻³ (per islet volume) [18] was used. Moreover, a dirac step was incorporated to stop oxygen consumption in areas where oxygen levels fell below the critical oxygen tension, $C_{cr} = 1e-4$ mol/m³, as developed by Buchwald et al [18].

The model consisted of two subdomains: *i*) the suspension medium; and *ii*) the spherical islets. Islets of variable sizes were used, i.e. 100–150 and 200–250 μm in diameter, with the distribution based on data collected for islet isolations used in these experiments. The total surface area of islets was 150 IEQ/cm² for standard islet density cultures and 1330 IEQ/cm² for high islet density loadings. The oxygen diffusion coefficient was assumed to be 3×10^{-9} m²/s in both domains [18]. An initial ($t = 0$) oxygen concentration of 0.2 mM (representing standard incubator oxygen tension) was assumed for the two subdomains. A boundary condition at the top of subdomain *i* was implemented to model the external oxygen

concentration of the culture system, with 0.01 mM for low oxygen and 0.2 mM for standard oxygen. Insulation and no flux was assumed for the walls of the insert. Finally, an inward flux boundary condition was implemented at the bottom of subdomain i to represent the oxygen release rate from OxySite. This flux boundary was calculated from average release kinetics of OxySite disks performed using sealed noninvasive oxygen release chambers over 3 days (Instech Laboratories, PA) [15]. After completion of modeling, to summarize the impact, the area (%) of the islet domain that experienced oxygen tensions that would result in either nonviable ($C_{CR-VIABILITY} = 1 \times 10^{-4}$ mM) or nonfunctional (classified as oxygen tensions whereby expected insulin secretion was significantly impacted, e.g. $C_{CR-INSULIN} = 5.1 \times 10^{-4}$ mM) islets was calculated [20]. Of note, models were generated using boundary conditions of theoretical oxygen tensions in standard incubators for the standard oxygen control; however, experimental oxygen tensions at the periphery of the culture dish were significantly lower, resulting in increased impact on islet viability and function.

2.4 Oxygen Studies with Pancreatic Islets

Based on mathematical modeling data, 1500 IEQ were seeded within Millicell inserts in 24-well plates (1330 IEQ/cm^2) and supplemented with CMRL (700 μL). Islets were incubated at either 0.2 mM (20%) O_2 (**0.2 mM Control**) or 0.01 mM (1%) O_2 (**0.01 mM Control**) or at 0.01 mM O_2 with an OxySite disk (**OxySite**). Low oxygen cultures were steadily maintained using a Hypoxia Chamber (Biospherix). Controls groups received a blank PDMS disk. An additional control of islets cultured at 150 IEQ/cm^2 density and 0.2 mM oxygen (**Free Islets**) were included in selected assessments for reference. Groups were incubated for up to 24 h, depending on the study. The culture media oxygen tensions were validated using oxygen sensors (Presense) suspended in the culture media of cell-free wells and incubated under the defined conditions of 0.2 or 0.01 mM oxygen with or without an OxySite disk. Readings were recorded from 3 independent wells for up to 24 h.

2.5 In Vitro Cellular Assessments

Metabolic activity was assessed via MTT (Promega), as published [15]. Briefly, samples were incubated in fresh CMRL (250 μL) with MTT (28 μL) for 1 h. Stop solution (185 μL) was then added and incubated for 48 h. Absorption was measured at 570 nm using a microplate reader (Molecular Devices).

Islet function was assessed via a dynamic glucose-stimulated-insulin-release (GSIR) using a perfusion machine (Biorep), as described [21]. Islets (75 handpicked) were stimulated according to the following series: 10 min low glucose (3 mM), 20 min high glucose (11 mM), 15 min low glucose, 5 min KCL (25 mM), and 15 min low glucose. Insulin concentration was measured using an insulin ELISA (Mercodia). Lactate dehydrogenase (LDH) release was quantified as published [15]. Briefly, 100 μL of supernatant was mixed with 100 μL of working reagent (Cytotoxicity Detection Kit, Roche) and incubated for 30 min at RT. Stop solution (50 μL of 1 N HCl) was added and absorbance was measured at 492 nm.

Gene expression profiling was performed using PCR arrays. Total RNA was extracted and reverse transcribed using RNase Easy and RT2 First Strand Kits (Qiagen), following

manufacturer's instructions. PCR arrays (RT2 profiler PCR arrays Hypoxia Signaling and Inflammatory Cytokines & Receptors, Qiagen) were assessed using a QuantiStudio 6 flex (Life Technologies). For qRT-PCR, total isolated RNA (mirVana miRNA Isolation kit, Ambion) was reverse transcribed using High Capacity cDNA Reverse Transcription Kit (Invitrogen). Relative gene expression (see Table S1 for primers) was quantified using Taqman assays in a StepOne plus cyclor (Applied Biosystems), normalized against β -actin for rodents and 18 S for NHP. For both gene analysis relative expression was calculated by the C_t method and data represented as fold change from **0.2 mM controls**.

Secreted inflammatory cytokines and chemokines (MIP1a, MCP1, IL8, VEGFa, and IL-6) in the culture media were evaluated via Milliplex multiplex kits (EMD Millipore) using a Luminex xMAP following manufacturer's instructions.

Live/Dead samples were visualized using the Viability/Cytotoxicity Kit (Invitrogen) and a Leica SP5 inverted confocal microscope, as described previously [15]. After incubation, samples were imaged for live cells (green) and dead cells (red). Z stacks (1 μ m thickness; 10 slices per image; 1024 \times 1024; 20 \times objective) were merged into a 3D projection using LAS lite Leica Software.

Immunohistochemical analysis of hypoxic dyes in culture islets was performed 24 h post hypoxic exposure for **0.01 mM Control** and **OxySite** samples. Pimonidazole solution (20 μ l at 1mg/mL; Hypoxyprobe) was added to the media, in the insert, and samples were placed back in the hypoxic chamber for an additional 2 h. After incubation, samples were removed, fixed in 10% formalin and stained in suspension for insulin (Dako A0564, 1:100), and glucagon (Abcam ab10988, 1:50). Histological images were collected using a Zeiss LSM 510 confocal microscope. Islet oxygen consumption rate (OCR) was measured using custom 4-chamber oxygen sensing chambers (Instech), similar to previous report [22]. In short, 250 IEQ were resuspended in 1 mL of pre-warmed CMRL, loaded into the chamber, and sealed. Recorded OCR was normalized to DNA concentration per sample (Quant-iT PicoGreen dsDNA kit, Invitrogen). Islet respirometry assessments were performed as described previously [23]. Briefly, islets were transferred to XF media (3 mM glucose, 1% FBS without HEPES; Seahorse Bioscience), loaded into a XF24 plate (70 islets/well; n = 3/group), and incubated for 1 h at 0% CO₂, 37 °C before placing in respirometry machine (Seahorse Bioscience). OCR was measured at basal (3 mM) and high (11 mM) glucose levels and normalized to DNA concentration per sample. The shift in OCR from basal to high glucose (OCR_{glc}) was calculated. Data is expressed as mean \pm SEM.

2.6 Islet Transplant and Graft Assessment

Lewis female rats recipients received 2 intraperitoneal injections of 60 mg/kg streptozotocin and were only used as recipients after 3 consecutive readings of non-fasting blood glucose levels > 350 mg/dL. Islets (1800 IEQ) were cultured for 24 h prior to transplant at **0.2 mM Control** or **0.01 mM OxySite**. Islets were collected from culture dishes using a Hamilton syringe and transplanted into the omentum following methods previously described [16]. Briefly, islets were gently loaded on top of the spread rat omentum and fibrin hydrogel (7.5 μ L fibrinogen solution; 8 mg/mL; added to 7.5 μ L of thrombin solution; thrombin (2 U/mL), aprotinin (85 mg/mL), 5 mM CaCl₂, 150 mM NaCl, and 20 mM HEPES) was added on top

of the islets to keep them in place. Excess omentum was then folded over the islet/fibrin graft and the edges were sealed using the same fibrin gel to generate an omental pouch (OP).

Normoglycemia was defined as stable nonfasting glycemic levels < 200 mg/dL for at least three consecutive blood glucose (BG) readings [16]. For metabolic assessment of grafts, an intravenous glucose tolerance test (IVGTT) was performed at 30 d post-transplant on selected animals, as previously described [16]. Briefly, after overnight fasting, rats received a glucose bolus (IV; 2 ul 50% dextrose / g BW) and BG levels were monitored until reading < 200 mg/dL or after 100 mins. The area under the curve (AUC) of glucose was then calculated [16]. To ensure observed normoglycemia was due to the islet graft and not residual native pancreas function, the islet-loaded omentum was removed in a survival surgery and the animal BG was monitored for a minimum of 3 d.

Explanted grafts were fixed in 10% formalin and embedded in paraffin blocks for immunohistochemical analysis. Slides were stained for insulin (Dako A0564, 1:100), SMA (Abcam ab5694, 1:50), glucagon (Abcam ab10988, 1:50), and DAPI (Invitrogen D1306, 1:500), as described elsewhere [16]. Histological images were collected using a Zeiss LSM 510 confocal microscope.

2.7 Statistical Analysis

Comparisons between groups were made using the same islet preparation with $n = 3$ for each measurement. Unless indicated, values are mean \pm SD. A minimum of 3 independent islet isolations were performed to confirm trends, with the exception of gene microarrays, OCR, and respiratory measurements, which was collected from 1 islet isolation. Statistical analysis was performed using the Student's *t* test or two-way ANOVA. Post-hoc analysis for multiple comparisons was done using a Bonferroni-Holm test. Statistical significance was considered at $P < 0.05$.

3. Results

3.1 OxySite Dampens Activation of Hypoxia Inducible Factors and Preserves Islet Viability

To evaluate the impact of OxySite on alleviating hypoxia-induced islet death and dysfunction, a time-course *in vitro* study was performed, where islets were co-cultured with either PDMS control disks or OxySite disks (10 mm diameter; Figure 1B), as schematically represented in Figure 1A. To first characterize oxygen kinetics with or without OxySite, oxygen trace measurements were collected from acellular cultures containing a PDMS control or OxySite disk and incubated under standard oxygen (0.2 mM) or low oxygen (0.01 mM) conditions for 24 h. As shown in Figure 1C, oxygen measurements validated deprived oxygen conditions in the **0.01 mM Control** group ($0.01 \pm 8.3e-4$ mM). Oxygen readings of media incubated under **0.2 mM Control** conditions averaged $0.15 \pm 3e-3$ mM; slightly lower than the set ambient gas level but consistent with published reports [24]. The supplementation of 0.01 mM oxygen cultures with an OxySite disk (**OxySite** group) resulted in oxygen levels as high as 0.3 ± 0.02 mM during the 24 h culture time.

To accurately capture the oxygen gradients experienced by the islets under the various culture conditions, 2-D multiphysics modeling was employed. In this approach, the external

oxygen tension set by the incubator, the oxygen generated by the OxySite material, and the oxygen consumed by the metabolically active islets was incorporated into the model. As oxygen diffusional limitations worsen in proportion to islet volume, a range of islet sizes, matched to our average rat islet isolation distribution, was included to generate a more predictive model [18]. Further, the external oxygen tension (incubator oxygen) and islet culture density (IEQ/cm² culture area) was manipulated to mimic conditions more relevant to the transplant setting [25]. As shown in Figure 2, computational models of standard (150 IEQ/cm²) and high (1,330 IEQ/cm²) islet loading densities under standard (0.2 mM) oxygen conditions predicted no detrimental oxygen gradients, with oxygen values for high density controls ranging from 6×10^{-3} to 0.15 mM (Figure 2 A–B). Contrariwise, the combination of high islet loading density and low oxygen conditions resulted in hypoxia for 46% of the islet mass, as defined by oxygen tensions levels below that which is supportive of islet viability (i.e. 1×10^{-4} mM) after only 8 h of culture (Figure 2C; hypoxic areas represented in black). This was more notable for the larger diameter islets (250 μ m), as illustrated by the variation of oxygen gradient along the islet clusters. Conversely, the introduction of OxySite to this culture system resulted in supportive oxygen tensions with an oxygen gradient ranging from 0.8×10^{-4} to 0.13 mM; resulting in the prediction of no hypoxic regions (Figure 2 D–E). The comparison of oxygen tensions for the OxySite group to the 0.2 mM Control group (Figure 2 B–D) found similar oxygen ranges, albeit islets in the OxySite treated group were predicted to experience marginally lower oxygen tensions than standard oxygen controls. As islets can remain viable but lose their responsiveness to glucose within interim oxygen tensions (i.e. less than 5.1×10^{-4} mM), the potential of this interim oxygen tension to impact insulin secretion was characterized. As shown in (Figure 2E), models predict impaired insulin secretion for 100 % of the islets cultured under 0.01 mM after 24 h, whereby 54% of OxySite-treated low oxygen culture islets should exhibit this deficiency.

Based on these computational predictions, pancreatic islets were cultured for up to 24 h at a loading density of 1,330 IEQ/cm² under standard incubator (**0.2 mM Control**) or low (**0.01 mM Control**) oxygen culture conditions. To provide oxygen supplementation, a single OxySite disk was added to the low oxygen cultures (**OxySite**). Rat pancreatic islets were the primary type studied; however, nonhuman primate islets were screened to validate observations in a species more closely resembling human islets [26]. Of note, concurrent characterization of potential cytotoxic byproducts of the calcium peroxide reaction, e.g. hydrogen peroxide and hydroxyl radical (OH⁻), found no significant changes in pH (Figure S1A) and only a modest elevation in H₂O₂ that was well below reported cytotoxic levels (Figure S1B) [27, 28]. As such, supplementation of OxySite cultures with scavenging agents, such as catalase, was not needed.

Initial immunohistochemical analysis of whole islets following exposure to the defined culture conditions validated our theoretical model predictions, whereby the low oxygen culture group (**0.01 mM Control**) depicted increased accumulation of hypoxia sensitive dyes, while hypoxyprobe staining within standard oxygen cultures (**0.2 mM Controls**) and low oxygen plus OxySite (**OxySite**) cultures was minimal (Figure 3). Further characterization via gene expression profiling indicated hypoxic pathway activation for low oxygen cultures (**0.01 mM Control**; Figure 4A), with strong upregulation of *HIF-1 α* and its

downstream regulators (*Arnt*, *Per1*, *Hnf4a* and *Cops5*) after both acute (8 h) and chronic (24 h) exposure. The second-phase HIF gene, *HIF-3a*, and its downstream targets (*Nrdg1* and *Ruvbl2*) were also prominently upregulated. *OxySite* treated cultures still exhibited upregulation of markers associated with *HIF-1a* stabilization; however, second phase HIF genes were not impacted and were, in fact, downregulated when compared to the **0.2 mM Control** group. A major consequence of accumulation of HIFs is the activation of deleterious apoptotic pathways [8]. *OxySite* treated cultures displayed a switching in gene expression from pro-apoptotic (e.g. *Bnip3*, *Bnip3l*, *Ddit4*, *eNos*, and *Adm*) to anti-apoptotic (*Ler3* and *Pim1*), when compared to both **0.01 and 0.2 mM Control** groups (Figure 4A).

The observed activation of *HIF-1a* and its downstream apoptotic gene pathways in the **0.01 mM Control** group resulted in the significant decrease in overall islet metabolic activity (29.8 and 59.6% decrease for 8 and 24 h, respectively) (Figure 4B). This was in stark contrast to *OxySite* treated islets, which were higher than even the **0.2 mM Controls**. Observations were validated using Live/Dead imaging (Figure 4C), where evidence of rat islet fragmentation and increased cell death in low oxygen cultures emerged after only 8 h. Conversely, robust, intact, and viable islets were found for the *OxySite* group at all time points.

Similar trends in preservation of islet viability using *OxySite* were also observed for NHP islets (Figure S2). Activation of apoptotic pathways was quantified via expression of BCL-2 family pro-apoptotic markers. Intriguingly, *Bax* was significantly upregulated in the *OxySite* group at 8 h, compared to both controls, but reversed at 24 h.

3.2 *OxySite* Reduces the Activation of Anaerobic Glycolysis and its Downstream Effects

It has been well-documented that hypoxic stabilization of *HIF-1a* results in the transcription of glucose transporters (*Glut1* and *Glut2*) and glycolytic enzymes, such as *Pgk1* [29]. Gene expression profiling of **0.01 mM Control** islets demonstrated an expected upregulation of all enzymes involved in the breakdown of glucose and for glucose transporters (Figure 5A). This enhanced expression, together with the accumulation of downstream by-products of glycolysis such as *Ldh* and *Pdk1*, suggests a prominent shift to anaerobic glycolysis [29]. Supplementation with *OxySite* reversed this phenotype, indicating retention of electron transport respiration for this group. Trends were validated using qPCR (Figure 5B–D), with significant downregulation of *Glut1*, *Pgk1*, and *Ldh* observed for the *OxySite* group, even when compared to **0.2 mM Control**. LDH protein secretion analysis validated qPCR trends.

Evaluation of pancreatic islet intracellular ATP concentrations and oxygen respiration served to confirm the degree of hypoxia in the tested groups (Figure S3). Low oxygen cultured islets exhibited a reduction in both ATP production and oxygen consumption rate (OCR), while the addition of *OxySite* not only restored but increased ATP and OCR levels above the **0.2 mM Control** (Figure S3 A–B). Delineation of the influence of hypoxia on beta cells via glucose challenge indicated an even more pronounced impact of *in situ* oxygenation (Figure S3 C–D), whereby *OxySite* islets exhibited over a 3.5-fold increase in OCR_{glc} when compared to even the **0.2 mM Control**.

A critical impact of hypoxia on pancreatic islets is the loss of insulin transcription and responsiveness to glucose stimulation due to mitochondrial dysfunction [8]. For this purpose, a dynamic glucose-stimulated-insulin-release test was conducted (Figure 6A–B). Islets cultured under low oxygen for 8 h demonstrated a limited response to high glucose stimulation, with a single, late, and unsustained peak near the end of the stimulation period; however, intracellular insulin content, as observed by islet depolarization via KCl stimulation, appeared substantial (Figure 6D). By 24 h, low oxygen cultured islets exhibited a complete loss of glucose responsiveness and minimal insulin content, with impaired KCl-stimulated insulin release. Alternatively, **OxySite** treated islets retained glucose responsiveness after 8 h of culture, with prompt, biphasic stimulation during high glucose challenge and significantly robust insulin release following depolarization ($P = 0.010$ vs **0.01 mM Control**). While the first phase peak for the **OxySite** group was dampened after 24 h, this did not impact overall responsiveness, as the AUC was statistically comparable to 8 h ($P = 0.11$; Figure 6C). Total insulin content was impacted at 24 h ($P = 0.033$), but was significantly higher than low oxygen controls ($P = 0.0001$).

A similar influence of low oxygen tension and the presence of OxySite on glucose processing was observed for NHP islets, with decreased activation of *Glut1*, *Pgk1*, and *Ldh* genes and LDH protein release for NHP **OxySite** treated islets (Figure S4).

3.3 OxySite Diminishes Hypoxia Induced Inflammatory Markers in Pancreatic Islets

Hypoxic stress is tightly coupled to elevated activation of inflammatory pathways via HIF-1 α activated NF- κ b signaling [30]. Likewise, islet metabolic stress can result in a 60–80% increase in the generation of potent islet-derived pro-inflammatory cytokines [31]. Investigation of the impact of OxySite on hypoxia-induced expression and secretion of inflammatory markers found decreased activation of several inflammatory factors associated with low oxygen culture, including *Ifng*, *Il17a*, *Cxcl2*, *Ccr2*, and *Cxcr2* (Figure 7A), after 8 h. This suppression became more pronounced after 24 h, with 8 of the 15 genes studied downregulated, even when compared to the **0.2 mM Control**.

A more in-depth qPCR analysis of the inflammatory effector *iNos* found all groups exhibited comparable upregulation at 8 h, but significant downregulation for the **OxySite** group at 24 h, when compared to both controls. Interestingly, *iNos* expression was also downregulated in the **0.01 mM Control** group, when compared **0.2 mM Control** (Figure 7B). Further, PCR quantification of *Ccl2* revealed trends similar to microarray data, with expression highest for islets cultured with **OxySite** at 8 h; however, after 24 h, the **OxySite** group was comparable to **0.2 mM Control**, while low oxygen controls were elevated (Figure 7C).

Moreover, the secretion of inflammatory factors, IL6, IL-8, CCL2, and MIP-1 α was measured via multiplexing. A significant elevation in MIP-1 α was observed after 24 h culture in low oxygen, when compared to those supplemented with OxySite or standard oxygen cultures (Figure 7D). Conversely, the **OxySite** group exhibited a significant elevation in CCL2 release, compared to both **0.01** and **0.2 mM Control** groups, at both time points (Figure 7E). No change in IL-6 or IL-8 release was observed between groups (Figure 7F–G).

Characterization of inflammatory pathways of NHP islets validated aforementioned observations (Figure S5), whereby elevated secretion of CCL2 was observed for *OxySite* treated islets at 8 h, with reversal of this trend after 24 h. Moreover, elevated IL-8 and IL-6 release for *0.01 mM Control* NHP islets was detected after 24 h, when compared to both *OxySite* and *0.2 mM Control*.

3.4 Co-culture of Islets with OxySite Does Not Hamper Islet Angiogenic Potential

Of particular interest in the development of strategies to alleviate HIF-1 α downstream pathways is its potential impact on neovascularization. A screening of pro-angiogenic genes (Figure 8A) demonstrated upregulation of major HIF-induced pro-angiogenic factors (*Vegfa*, *Pgf*, *Angptl4*, and *anxa2*), as well as some of their respective downstream regulators (*Lox*, *Hmox1*, *Jmjd6*, *Serpine1*, and *Mmp9*), after 8 h of low oxygen exposure. This trend was sustained and even elevated for selected factors after 24 h. The addition of OxySite led to downregulation of most of these genes. The quantification of *Vegfa* mRNA expression and subsequent VEGF protein secretion (Figure 8B–C), however, revealed contrary trends. While significant downregulation of *Vegfa* was quantified for both the *0.01 mM Control* and *OxySite* group after 8 h, this trend was not fully translated to protein release, as VEGFa levels were significantly higher for the *OxySite* group than both *0.01* and *0.2 mM Control* groups at both time points. As protein studies examine cumulative release, it is reasonable to suspect that early upregulation of *Vegfa* in the *OxySite* group (e.g. < 8 h) could lead to these results. Further, qPCR analysis of *Vegfa* gene activation in the *0.01 mM Control* group measured downregulation for all time points studied, when compared to *0.2 mM Control*. This result was inconsistent with microarray data; however, the robust nature of the qPCR analysis (3 vs 1 isolation) favors these conclusions.

Validation of results for NHP islets lead to similar conclusions, although gene expression data indicate greater sensitivity to culture conditions (Figure S6). Specifically, *Vegfa* was upregulated for both *0.01* and *0.2 mM control* cultures at both 8 and 24 h time points, while *OxySite* treated islets exhibited significant downregulation ($P < 0.0001$ at both time points). As with rat islets, gene expression profiles did not mirror cumulative protein release, as VEGFa protein media levels were inverted, with the highest VEGFa concentration observed for the *OxySite* group. Nevertheless, results indicate that treatment of hypoxic islets with OxySite did not impair VEGFa release.

3.5 Co-culture of Islets with OxySite Results in Enhanced Functional Outcomes

The impact of oxygen culture conditions on islet graft efficacy was tested using a syngeneic diabetic rat model. Examination of *in vitro* results for low oxygen culture groups (e.g. *0.01 mM Control* and *0.01 mM OxySite*) indicated that the *0.01 mM Control* group would not be suitable for testing *in vivo*, as these islets were nonfunctional (e.g. nonresponsive to a glucose challenge). As such, to provide a more rigorous comparison, the *0.01 mM OxySite* group was directly compared to the *0.2 mM Control* group. Islets were cultured under either of these defined conditions for 24 h prior to transplantation into the extrahepatic omental pouch (OP) site, using methods previously published and similar to on-going clinical trials (P.I. Rodolfo Alejandro, [clinicaltrials.gov](https://clinicaltrials.gov/ct2/show/study/NCT02213003): NCT02213003) [16, 32].

Within the first 10 days post-transplantation, stabilization to euglycemia was observed in 63% (5 out of 8) of the diabetic recipients of **OxySite** treated islets (Figure 9A), with these grafts remaining stable until elective OP removal 40 days post-transplant. Following graft removal of these functional implants, restoration to hyperglycemia was observed in these animals, verifying that diabetes reversal was due to the transplanted islets. The remaining 3 **OxySite** treated recipients exhibited blood glucose levels that fluctuated between 100 and 300 mg/dL. This was in stark contrast to recipients of **0.2 mM Control** islets, whereby 0% (0 out of the 8) reverted to normoglycemia and all exhibited blood glucose levels exceeding 250 mg/dL.

To further assess engraftment potency, an IVGTT was performed on recipients of **OxySite** treated islets (n = 5) or control islets (n = 3), with a nondiabetic animal used for metabolic reference. Animals transplanted with **OxySite** treated islets cleared glucose in a manner similar to naïve animals (AUC = 8677 ± 505 vs AUC= 7505) (Figure 9B). As expected, nonstable recipients of control islets failed to clear glucose in an effective manner (AUC = 25496 ± 7584, P = 0.019 vs **OxySite**).

Immunohistochemical analysis for insulin, glucagon, and SMA on explanted grafts for **OxySite** treated islets revealed preserved cytoarchitecture with insulin-positive beta cells, surrounded by glucagon-positive alpha cells and intra-islet SMA staining, indicating intra-vascularized islets within the omentum tissue (Figure 9C). In contrast, control grafts exhibited smaller and/or fragmented islets that lacked the architecture and organization of the treated group, although insulin and glucagon positive cells and SMA-positive tubules were observed.

4. Discussion

Inadequate oxygenation during *in vitro* culture and after *in vivo* intraportal transplantation has been recognized as a major factor contributing to decreased islet survival during culture and significant graft loss following implantation [33–35]. During the pre-transplant culture period, islets are exposed to detrimental oxygen gradients that can result in significant declines in viability and function [36]. To fully alleviate these gradients using standard culture dishes would require the application of impractical culture methods [36, 37]. While advancements have been made in modifying culture flasks to enhance oxygen permeability [37], the implementation of *in situ* oxygen generators has the potential to heighten the viability of islet tissue and provide a more practical and cost effective method for improving *in vitro* culture, as oxygen supplementation could be tailored to the cellular demand of the tissue. As it relates to transplant outcomes, these materials could be conveniently translated *in vivo*; providing local and controlled augmented oxygen.

Oxygen deprivation is regulated by hypoxia inducible factors (HIFs), which are tightly controlled proteins that depend on oxygen gradients for their translocation and stabilization [38, 39]. Herein, we set to investigate the effects of our oxygen generating material in the activation of HIF controlled pathways *in vitro*. Both low oxygen and **OxySite** treated islets demonstrated gene activation of HIF-1 α and its dimer ARNT (also known as HIF-1 β). Activation of HIF-1 α in the **OxySite**-treated cultures may read contradictory; however,

HIF-1 α upregulation under normoxia (i.e. not due to oxygen insufficiency) has been observed in the presence of reactive oxygen species, such as H_2O_2 , as they are implicated in the signaling process [40]. Further, recent publications hint at a role of HIF-1 complex in β -cell metabolism and insulin responsiveness [6, 38, 39]. Thus, the modest activation of HIF-1 α in OxySite cultures, either by the mild accumulation of H_2O_2 or by enhanced oxygen consumption, could potentially improve insulin secretion without imparting negative effects. This is further supported by the observed downregulation of HIF-3 α and its target pro-apoptotic pathways in OxySite cultures, compared to both low oxygen and standard oxygen controls. These results, together with the subsequent preservation of metabolic activity and viability, indicate that OxySite can significantly mitigate key markers associated with hypoxia-induced islet loss, while not hindering β -cell homeostasis.

Reprogramming of cellular metabolism is a critical adaptive response to oxygen and nutrient deprivation in models of ischemic insults in diabetic patients [41]. HIF-1 α plays a prominent role in glucose catabolism and cellular oxidative responses in hypoxic settings by promoting the expression of glucose transporters, glycolytic enzymes, and lactate dehydrogenase [42, 43]. Glycolytic and enzymatic markers that direct a shift toward anaerobic glycolysis were identified in islets cultured at low oxygen conditions. This shift also led to dampened cellular respiration. Supplementation with OxySite, however, demonstrated the ability of our oxygen generator to support aerobic respiration and preserve OCR, even under chronic low oxygen conditions (24 h). Preventing anaerobic glycolysis and preserving islet and beta cell respiration likely contribute to the observed improved graft outcomes for OxySite treated islets, as anaerobic pathways negatively impact β -cell function and insulin transcription, while dampened OCR correlates to poor transplant efficacy [44].

Comparing our experimental results to our theoretical predictions indicates that our multiphysics model undervalued the influence of OxySite on islet function and viability, whereby OxySite treated islets cultured under low oxygen tensions exhibited minimal activation of hypoxia-induced pathways. This difference might be explained by an underestimation of the OxySite's oxygen kinetics, which was measured using acellular cultures. Given that islets will generate a continuous oxygen sink, the kinetics of the OxySite reaction may be elevated as the end product, oxygen, is consumed.

Early graft loss has also been linked to non-specific inflammation around the graft, which is unrelated to specific host immune responses [45]. Previous studies have shown that concomitant activation of HIF-1 α and NF κ B regulates activation of pro-inflammatory genes under hypoxia [46]. Microarray data found OxySite to suppress hypoxia-induced activation of several potent inflammatory regulators and effectors, notably *Infg*, *Il-17*, and *Il-6*, which play prominent roles in the activation of beta cell's "extrinsic" apoptotic pathway [47, 48]. As such, downregulation of these factors can lead to a significant positive impact on islet health and clinical efficacy. OxySite also promoted the downregulation of *iNos*; a potent player in the generation of oxidative stress and cytokine induced β -cell death [49]. Of interest, *iNos* was not upregulated in the low oxygen control group after 24 h of culture; however, activation of *iNos* under strict hypoxia has been reported to be minimal and require complimentary cytokines, such as Il-1b, to elevate expression [50]. Finally, upregulation of both gene and protein expression of CCL2 was noted in our OxySite co-culture system.

While CCL2 expression *in vivo* has been associated with elevation of damaging cellular infiltrates [51], recent evidence suggests a protective role via promotion of tolerogenic dendritic cell migration to the graft [52]. Moreover, CCL2 has been correlated with enhanced glucose responsiveness and the regeneration of the peri-islet capsule post-isolation [53]. Thus, the role of CCL2 under our oxygenated cultures is an interesting aspect that requires further investigation.

The role of HIF-1 α in the vascular response has been well documented in the literature, in particular its effect on angiogenic genes such as VEGF [54]. Thus, limiting the ability of HIF-1 α to activate these pathways via oxygen supplementation might appear counterproductive. In this study, however, severe hypoxia was not found to induce VEGF protein release from islets. While seemingly contrary to other published reports [55], the degree of hypoxia-induced damage observed in low oxygen controls in this study suggests that, in the face of severe oxygen deprivation, there is a shift towards conservation that hinder the stable translation of pro-angiogenic agents. This trend is supported by literature demonstrating a general suppression of mRNA transcription, including VEGF [56, 57], and a reduction of the angiogenic capacity of isolated islets [58], after chronic hypoxia. Thus, the incorporation of OxySite to prevent islet hypoxia should not impair the efficiency or competency of the resulting vascular network.

Condensed *in vitro* assessments conducted using NHP islets demonstrated trends comparable to that observed for rat islets, with preservation of islet architecture, viability, mitochondrial glucose oxidation, and angiogenic potential for the OxySite treated group. Interestingly, *Bax* levels were initially upregulated for OxySite and standard oxygen control groups (8 h), although this was not sustained. While BCL-2 proteins are typically associated with pro-apoptotic regulation, recent evidence suggests that they may play dual roles in balancing stimulation of apoptosis with islet metabolism and insulin secretion coupling [59]. As such, the activation of *Bax* in our oxygenated cultures could be associated with the observed elevated metabolic activity. With respect to cytokine activation, NHPs demonstrated elevated sensitivity to hypoxia, with a significant increase in the release of pro-inflammatory cytokines Il-6 and Il-8 in low oxygen controls. The capacity of OxySite to inhibit the expression of these cytokines, which contribute to delayed glucose responsiveness, induce direct β -cell toxicity, and lead to the recruitment and activation of host immune cells [60], should result in beneficial effects on islet engraftment and long-term acceptance.

The favorable islet health profile promoted by the culture of islets with OxySite resulted in a significant impact in overall graft efficacy, whereby OxySite treated islets cultured under hypoxic conditions outperformed islets cultured under standard oxygen tensions. Further, the strong intra-islet vascularization observed for OxySite treated islets corroborates that healthy islets result in strong graft engraftment. Altogether, these results highlight the importance of oxygen in the preservation of islets in culture, particularly when islet yields are unpredictable and have a strong correlation to overall clinical efficacy [61, 62].

With evidence that generating favorable oxygen gradients *in vitro* elevates islet health, future efforts are focused on increasing the poor oxygenation of islet grafts *in vivo* [12]. While the

graft microenvironment has been improved via better transplant sites and enhanced revascularization [63], few approaches are focused on providing *in situ* oxygenation. Recent promising publications highlight the potential of oxygen supplementation for improved graft viability [64, 65]; however, these approaches, which utilize a refillable oxygen tank system, require cumbersome external ports and high patient compliance to provide indefinite oxygen supplementation. In this approach, OxySite can provide ease of incorporation with no patient interface. Further, due to the low adherence of the PDMS material, OxySite could easily be removed and replaced to provide long-term oxygen delivery [66]. As an alternative approach, combining short-term oxygen supplementation with macroporous scaffolds can offer a supportive microenvironment to bridge the transplant from an avascular implant to a competent vascularized graft [16, 67–70]. This approach could protect islets during their most vulnerable period, thereby providing the necessary boost to improve not only early, but late stage, efficacy.

5. Conclusion

The work presented herein demonstrates the capacity of OxySite to provide a cost effective, spatially favorable, *in situ* oxygenator to support pancreatic islet culture. The addition of OxySite to high cell density and physiologically relevant oxygen cultured resulted in the mitigation of metabolic burnout, apoptotic activation, and the release of pro-inflammatory cytokines, while preserving islet health, as validated by conserved insulin release profiles and oxygen consumption rates. Further, the inclusion of OxySite had no deleterious effect on the angiogenic potential of these cells. Finally, the capacity of *in situ* oxygenation, through OxySite, of pancreatic islet cultures to enhance the engraftment and subsequent functional outcomes of islet grafts *in vivo* was established. With these established benefits, this material has great potential to improve the survival of numerous cultured tissues prior to transplant. The incorporation of temporary *in situ* oxygenation into biomaterial scaffolds, engineered for housing islets within extrahepatic sites, is the focus of future studies [16].

Supplementary Material

Refer to Web version on PubMed Central for supplementary material.

Acknowledgments

This work was supported by the JDRF and Leona M. and Harry B. Helmsley Charitable Trust (3-SRA-2015-38-Q-R). Ms Coronel was supported by an F31 individual predoctoral fellowship (1F31DK097956-01). We thank Irayme Labrada for her excellent technical assistant during islet isolations and animal transplants. We thank Dr. Norma Kenyon and her team at the Diabetes Research Institute at the University of Miami, in particular Dr. Dora Berman and Alex Rabassa, for the isolation and characterization of NHP islets used in this study. C.L.S. is the guarantor of this work and, as such, had full access to all the data in the study and takes responsibility for the integrity of the data and the accuracy of the data analysis.

References

1. Shapiro AM, Ricordi C, Hering BJ, Auchincloss H, Lindblad R, Robertson RP, Secchi A, Brendel MD, Berney T, Brennan DC, Cagliero E, Alejandro R, Ryan EA, DiMercurio B, Morel P, Polonsky KS, Reems JA, Bretzel RG, Bertuzzi F, Froud T, Kandaswamy R, Sutherland DE, Eisenbarth G, Segal M, Preiksaitis J, Korbitt GS, Barton FB, Viviano L, Seyfert-Margolis V, Bluestone J, Lakey

- JR. International trial of the Edmonton protocol for islet transplantation. *N Engl J Med*. 2006; 355(13):1318–30. [PubMed: 17005949]
2. C.R. Group. 2007 update on allogeneic islet transplantation from the Collaborative Islet Transplant Registry (CITR). *Cell Transplant*. 2009; 18(7):753–67. [PubMed: 19796497]
 3. Barton FB, Rickels MR, Alejandro R, Hering BJ, Wease S, Naziruddin B, Oberholzer J, Odorico JS, Garfinkel MR, Levy M, Pattou F, Berney T, Secchi A, Messinger S, Senior PA, Maffi P, Posselt A, Stock PG, Kaufman DB, Luo X, Kandeel F, Cagliero E, Turgeon NA, Witkowski P, Naji A, O'Connell PJ, Greenbaum C, Kudva YC, Brayman KL, Aull MJ, Larsen C, Kay TW, Fernandez LA, Vantyghem MC, Bellin M, Shapiro AM. Improvement in outcomes of clinical islet transplantation: 1999–2010. *Diabetes care*. 2012; 35(7):1436–45. [PubMed: 22723582]
 4. Cantley J, Grey ST, Maxwell PH, Withers DJ. The hypoxia response pathway and beta-cell function. *Diabetes Obes Metab*. 2010; 12(Suppl 2):159–67. [PubMed: 21029313]
 5. Gribble FM. Intolerant of glucose and gasping for oxygen. *Nat Med*. 2009; 15(3):247–249. [PubMed: 19265823]
 6. Cheng K, Ho K, Stokes R, Scott C, Lau SM, Hawthorne WJ, O'Connell PJ, Loudovaris T, Kay TW, Kulkarni RN, Okada T, Wang XL, Yim SH, Shah Y, Grey ST, Biankin AV, Kench JG, Laybutt DR, Gonzalez FJ, Kahn CR, Gunton JE. Hypoxia-inducible factor-1 α regulates beta cell function in mouse and human islets. *J Clin Invest*. 2010; 120(6):2171–83. [PubMed: 20440072]
 7. Dionne KE, Colton CK, Yarmush ML. Effect of oxygen on isolated pancreatic tissue. *ASAIO Trans*. 1989; 35(3):739–41. [PubMed: 2688724]
 8. Moritz W, Meier F, Stroka D, Giuliani M, Kugelmeier P, Nett P, Lehmann R, Cadninas D, Gassmann M, Weber M. Apoptosis in hypoxic human pancreatic islets correlates with HIF-1 α expression. *The FASEB Journal*. 2002; 16(7):745–747. [PubMed: 11923216]
 9. Semenza GL. Regulation of mammalian O₂ homeostasis by hypoxia-inducible factor 1. *Annu Rev Cell Dev Biol*. 1999; 15:551–78. [PubMed: 10611972]
 10. Fraker CA, Cechin S, Alvarez-Cubela S, Echeverri F, Bernal A, Poo R, Ricordi C, Inverardi L, Dominguez-Bendala J. A physiological pattern of oxygenation using perfluorocarbon-based culture devices maximizes pancreatic islet viability and enhances beta-cell function. *Cell Transplant*. 2013; 22(9):1723–33. [PubMed: 23068091]
 11. Papas KK, Avgoustiniatos ES, Tempelman LA, Weir GC, Colton CK, Pisanía A, Rappel MJ, Friberg AS, Bauer AC, Hering BJ. High-Density Culture of Human Islets on Top of Silicone Rubber Membranes. *Transplantation Proceedings*. 2005; 37(8):3412–3414. [PubMed: 16298611]
 12. Carlsson PO, Palm F, Andersson A, Liss P. Markedly decreased oxygen tension in transplanted rat pancreatic islets irrespective of the implantation site. *Diabetes*. 2001; 50(3):489–95. [PubMed: 11246867]
 13. Olsson R, Olerud J, Pettersson U, Carlsson PO. Increased Numbers of Low-Oxygenated Pancreatic Islets After Intraportal Islet Transplantation. *Diabetes*. 2011; 60(9):2350–2353. [PubMed: 21788575]
 14. Mattsson G, Jansson L, Carlsson PO. Decreased vascular density in mouse pancreatic islets after transplantation. *Diabetes*. 2002; 51(1362–1366)
 15. Pedraza E, Coronel MM, Fraker CA, Ricordi C, Stabler CL. Preventing hypoxia-induced cell death in beta cells and islets via hydrolytically activated, oxygen-generating biomaterials. *Proceedings of the National Academy of Sciences of the United States of America*. 2012; 109(11):4245–50. [PubMed: 22371586]
 16. Pedraza E, Brady AC, Fraker CA, Molano RD, Sukert S, Berman DM, Kenyon NS, Pileggi A, Ricordi C, Stabler CL. Macroporous Three Dimensional PDMS Scaffolds for Extrahepatic Islet Transplantation. *Cell transplantation*. 2013; 22(7):1123–1135. [PubMed: 23031502]
 17. Kenyon NS, Chatzipetrou M, Masetti M, Ranuncoi A, Oliveira M, Wagner JL, Kirk AD, Harlan DM, Burkly LC, Ricordi C. Long-term survival and function of intrahepatic islet allografts in rhesus monkeys treated with humanized anti-CD154. *Proceedings of the National Academy of Sciences of the United States of America*. 1999; 96(14):8132–7. [PubMed: 10393960]
 18. Buchwald P. FEM-based oxygen consumption and cell viability models for avascular pancreatic islets. *Theor Biol Med Model*. 2009; 6:5. [PubMed: 19371422]

19. Avgoustiniatos ES, Colton CK. Effect of External Oxygen Mass Transfer Resistances on Viability of Immunoisolated Tissue. *Annals of the New York Academy of Sciences*. 1997; 831(1):145–166. [PubMed: 9616709]
20. Johnson AS, Fisher RJ, Weir GC, Colton CK. Oxygen consumption and diffusion in assemblages of respiring spheres: Performance enhancement of a bioartificial pancreas. *Chemical Engineering Science*. 2009; 64(22):4470–4487.
21. Buchwald P, Cechin SR, Weaver JD, Stabler CL. Experimental evaluation and computational modeling of the effects of encapsulation on the time-profile of glucose-stimulated insulin release of pancreatic islets. *BioMedical Engineering OnLine*. 2015; 14(1):1–14. [PubMed: 25564100]
22. Papas KK, Pisania A, Wu H, Weir GC, Colton CK. A stirred microchamber for oxygen consumption rate measurements with pancreatic islets. *Biotechnol Bioeng*. 2007; 98(5):1071–82. [PubMed: 17497731]
23. Wikstrom JD, Sereda SB, Stiles L, Elorza A, Allister EM, Neilson A, Ferrick DA, Wheeler MB, Shirihai OS. A Novel High-Throughput Assay for Islet Respiration Reveals Uncoupling of Rodent and Human Islets. *PLoS ONE*. 2012; 7(5):e33023. [PubMed: 22606219]
24. Bambrick L, Kostov Y, Rao G. In vitro cell culture pO₂ is significantly different from incubator pO₂. *Biotechnology progress*. 2011; 27(4):1185–1189. [PubMed: 21618722]
25. Weir GC, Bonner-Weir S, Leahy JL. Islet Mass and Function in Diabetes and Transplantation. *Diabetes*. 1990; 39(4):401–405. [PubMed: 2108068]
26. Cabrera O, Berman DM, Kenyon NS, Ricordi C, Berggren PO, Caicedo A. The unique cytoarchitecture of human pancreatic islets has implications for islet cell function. *Proceedings of the National Academy of Sciences of the United States of America*. 2006; 103(7):2334–2339. [PubMed: 16461897]
27. Maechler P, Jornot L, Wollheim CB. Hydrogen peroxide alters mitochondrial activation and insulin secretion in pancreatic beta cells. *Journal of Biological Chemistry*. 1999; 274(39):27905–27913. [PubMed: 10488138]
28. Fu-Liang X, Xiao-Hui S, Lu G, Xiang-Liang Y, Hui-Bi X. Puerarin protects rat pancreatic islets from damage by hydrogen peroxide. *European journal of pharmacology*. 2006; 529(1):1–7. [PubMed: 16321378]
29. Papandreou I, Cairns RA, Fontana L, Lim AL, Denko NC. HIF-1 mediates adaptation to hypoxia by actively downregulating mitochondrial oxygen consumption. *Cell Metab*. 2006; 3(3):187–97. [PubMed: 16517406]
30. Taylor CT, Cummins EP. The Role of NF- κ B in Hypoxia-Induced Gene Expression. *Annals of the New York Academy of Sciences*. 2009; 1177(1):178–184. [PubMed: 19845620]
31. Donath MY, Böni-Schnetzler M, Ellingsgaard H, Halban PA, Ehses JA. Cytokine production by islets in health and diabetes: cellular origin, regulation and function. *Trends in Endocrinology & Metabolism*. 2010; 21(5):261–267. [PubMed: 20096598]
32. Berman DM, Molano RD, Fotino C, Ulissi U, Gimeno J, Mendez AJ, Kenyon NM, Kenyon NS, Andrews DM, Ricordi C, Pileggi A. Bioengineering the Endocrine Pancreas: Intraomental Islet Transplantation Within a Biologic Resorbable Scaffold. *Diabetes*. 2016; 65(5):1350–1361. [PubMed: 26916086]
33. Lau J, Carlsson PO. Low revascularization of human islets when experimentally transplanted into the liver. *Transplantation*. 2009; 87(3):322–5. [PubMed: 19202435]
34. Mendoza V, Klein D, Ichii H, Ribeiro M, Ricordi C, Hankeln T, Burmester T, Pastori R. Protection of islets in culture by delivery of oxygen binding neuroglobin via protein transduction, *Transplantation proceedings*, Elsevier. 2005:237–240.
35. Papas KK, Karatzas T, Berney T, Minor T, Pappas P, Pattou F, Shaw J, Toso C, Schuurman HJ. Islet Transplantation without Borders Enabling islet transplantation in Greece with international collaboration and innovative technology. *Clinical transplantation*. 2013; 27(2):E116. [PubMed: 23330863]
36. Avgoustiniatos ES. Oxygen diffusion limitations in pancreatic islet culture and immunoisolation. *Massachusetts Institute of Technology*. 2002
37. Kitzmann, JP., Pepper, AR., Gala-Lopez, B., Pawlick, R., Kin, T., O’Gorman, D., Mueller, KR., Gruessner, AC., Avgoustiniatos, ES., Karatzas, T. Human islet viability and function is maintained

- during high-density shipment in silicone rubber membrane vessels, Transplantation proceedings. Elsevier; 2014. p. 1989-1991.
38. Bensellam M, Duville B, Rybachuk G, Laybutt DR, Magnan C, Guiot Y, Pouyssegur J, Jonas JC. Glucose-induced O₂ consumption activates hypoxia inducible factors 1 and 2 in rat insulin-secreting pancreatic beta-cells. *PLoS One*. 2012; 7(1):e29807. [PubMed: 22235342]
 39. Girgis CM, Cheng K, Scott CH, Gunton JE. Novel links between HIFs, type 2 diabetes, and metabolic syndrome. *Trends in Endocrinology & Metabolism*. 2012; 23(8):372–380. [PubMed: 22766319]
 40. Bell EL, Chandel NS. Mitochondrial oxygen sensing: regulation of hypoxia-inducible factor by mitochondrial generated reactive oxygen species. *Essays in biochemistry*. 2007; 43:17–28. [PubMed: 17705790]
 41. Beckman JA, Creager MA, Libby P. Diabetes and atherosclerosis: epidemiology, pathophysiology, and management. *JAMA*. 2002; 287(19):2570–81. [PubMed: 12020339]
 42. Cantley J, Grey ST, Maxwell PH, Withers DJ. The hypoxia response pathway and β -cell function. *Diabetes Obes Metab*. 2010; 12(Suppl 2):159–67. [PubMed: 21029313]
 43. Gordan JD, Thompson CB, Simon MC. HIF and c-Myc: sibling rivals for control of cancer cell metabolism and proliferation. *Cancer Cell*. 2007; 12(2):108–13. [PubMed: 17692803]
 44. Papas KK, Colton C, Nelson R, Rozak P, Avgoustiniatos E, Scott W, Wildey G, Pisania A, Weir G, Hering B. Human islet oxygen consumption rate and DNA measurements predict diabetes reversal in nude mice. *American Journal of Transplantation*. 2007; 7(3):707–713. [PubMed: 17229069]
 45. Nagata M, Mullen Y, Matsuo S, Herrera M, Clare-Salzler M. Destruction of islet isografts by severe nonspecific inflammation. *Transplant Proc*. 1990; 22(2):855–6. [PubMed: 2109420]
 46. Johansson U, Olsson A, Gabrielsson S, Nilsson B, Korsgen O. Inflammatory mediators expressed in human islets of Langerhans: implications for islet transplantation. *Biochem Biophys Res Commun*. 2003; 308:474–479. [PubMed: 12914774]
 47. Donath MY, Størling J, Maedler K, Mandrup-Poulsen T. Inflammatory mediators and islet β -cell failure: a link between type 1 and type 2 diabetes. *Journal of Molecular Medicine*. 2003; 81(8):455–470. [PubMed: 12879149]
 48. Campbell IL, Kay TW, Oxbrow L, Harrison LC. Essential role for interferon-gamma and interleukin-6 in autoimmune insulin-dependent diabetes in NOD/Wehi mice. *Journal of Clinical Investigation*. 1991; 87(2):739–742. [PubMed: 1899431]
 49. Chambers KT, Unverferth JA, Weber SM, Wek RC, Urano F, Corbett JA. The role of nitric oxide and the unfolded protein response in cytokine-induced β -cell death. *Diabetes*. 2008; 57(1):124–132. [PubMed: 17928398]
 50. Jung F, Palmer LA, Zhou N, Johns RA. Hypoxic Regulation of Inducible Nitric Oxide Synthase via Hypoxia Inducible Factor-1 in Cardiac Myocytes. *Circulation Research*. 2000; 86(3):319–325. [PubMed: 10679484]
 51. Grewal IS, Rutledge BJ, Fiorillo JA, Gu L, Gladue RP, Flavell RA, Rollins BJ. Transgenic monocyte chemoattractant protein-1 (MCP-1) in pancreatic islets produces monocyte-rich insulinitis without diabetes: abrogation by a second transgene expressing systemic MCP-1. *J Immunol*. 1997; 159(1):401–8. [PubMed: 9200479]
 52. Kriegel MA, Rathinam C, Flavell RA. Pancreatic islet expression of chemokine CCL2 suppresses autoimmune diabetes via tolerogenic CD11c⁺ CD11b⁺ dendritic cells. *Proc Natl Acad Sci U S A*. 2012; 109(9):3457–62. [PubMed: 22328150]
 53. Piemonti L, Leone BE, Nano R, Saccani A, Monti P, Maffi P, Bianchi G, Sica A, Peri G, Melzi R, Aldrighetti L, Secchi A, Di Carlo V, Allavena P, Bertuzzi F. Human pancreatic islets produce and secrete MCP-1/CCL2: relevance in human islet transplantation. *Diabetes*. 2002; 51(1):55–65. [PubMed: 11756323]
 54. Manalo DJ, Rowan A, Lavoie T, Natarajan L, Kelly BD, Ye SQ, Garcia JG, Semenza GL. Transcriptional regulation of vascular endothelial cell responses to hypoxia by HIF-1. *Blood*. 2005; 105(2):659–69. [PubMed: 15374877]
 55. Vasir B, Aiello LP, Yoon KH, Quicquel RR, Bonner-Weir S, Weir GC. Hypoxia induces vascular endothelial growth factor gene and protein expression in cultured rat islet cells. *Diabetes*. 1998; 47(12):1894–1903. [PubMed: 9836521]

56. Masuda K, Abdelmohsen K, Gorospe M. RNA-binding proteins implicated in the hypoxic response. *Journal of Cellular and Molecular Medicine*. 2009; 13(9a):2759–2769. [PubMed: 19583805]
57. McQuillan LP, Leung GK, Marsden PA, Kostyk SK, Kourembanas S. Hypoxia inhibits expression of eNOS via transcriptional and posttranscriptional mechanisms. *American Journal of Physiology - Heart and Circulatory Physiology*. 1994; 267(5):H1921–H1927.
58. Lai Y, Schneider D, Kiszun A, Hauck-Schmalenberger I, Breier G, Brandhorst D, Brandhorst H, Iken M, Brendel MD, Bretzel RG, Linn T. Vascular endothelial growth factor increases functional beta-cell mass by improvement of angiogenesis of isolated human and murine pancreatic islets. *Transplantation*. 2005; 79(11):1530–6. [PubMed: 15940042]
59. Luciani DS, White SA, Widenmaier SB, Saran VV, Taghizadeh F, Hu X, Allard MF, Johnson JD. Bcl-2 and Bcl-xL suppress glucose signaling in pancreatic β -cells. *Diabetes*. 2013; 62(1):170–82. [PubMed: 22933114]
60. Bottino R, Balamurugan AN, Tse H, Thirunavukkarasu C, Ge X, Profozich J, Milton M, Ziegenfuss A, Trucco M, Piganelli JD. Response of human islets to isolation stress and the effect of antioxidant treatment. *Diabetes*. 2004; 53(10):2559–68. [PubMed: 15448084]
61. Balamurugan AN, Naziruddin B, Lockridge A, Tiwari M, Loganathan G, Takita M, Matsumoto S, Papas K, Trieger M, Rainis H, Kin T, Kay TW, Wease S, Messinger S, Ricordi C, Alejandro R, Markmann J, Kerr-Conti J, Rickels MR, Liu C, Zhang X, Witkowski P, Posselt A, Maffi P, Secchi A, Berney T, O'Connell PJ, Hering BJ, Barton FB. Islet Product Characteristics and Factors Related to Successful Human Islet Transplantation From the Collaborative Islet Transplant Registry (CITR) 1999–2010. *American Journal of Transplantation*. 2014; 14(11):2595–2606. [PubMed: 25278159]
62. Ricordi C, Goldstein JS, Balamurugan AN, Szot GL, Kin T, Liu C, Czarniecki CW, Barbaro B, Bridges ND, Cano J, Clarke WR, Eggerman TL, Hunsicker LG, Kaufman DB, Khan A, Lafontant D-E, Linetsky E, Luo X, Markmann JF, Naji A, Korsgren O, Oberholzer J, Turgeon NA, Brandhorst D, Friberg AS, Lei J, Wang L-j, Wilhelm JJ, Willits J, Zhang X, Hering BJ, Posselt AM, Shapiro AMJ. NIH-sponsored Clinical Islet Transplantation Consortium Phase 3 Trial: Manufacture of a Complex Cellular Product at Eight Processing Facilities. *Diabetes*. 2016
63. Coronel MM, Stabler CL. Engineering a local microenvironment for pancreatic islet replacement. *Current Opinion in Biotechnology*. 2013; 24(5):900–908. [PubMed: 23769320]
64. Ludwig B, Reichel A, Steffen A, Zimmerman B, Schally AV, Block NL, Colton CK, Ludwig S, Kersting S, Bonifacio E, Solimena M, Gendler Z, Rotem A, Barkai U, Bornstein SR. Transplantation of human islets without immunosuppression. *Proc Natl Acad Sci U S A*. 2013; 110(47):19054–8. [PubMed: 24167261]
65. Ludwig B, Reichel A, Steffen A, Zimmermann B, Colton CK, Ludwig S, Kersting S, Bonifacio E, Solimena M, Gendler Z, Rotem A, Barkai U, Bornstein SR. Transplanting allo-islets without immunosuppression. *Xenotransplantation*. 2014; 21(2):189–189.
66. Mashak A, Rahimi A. Silicone polymers in controlled drug delivery systems: a review. *Iran Polym J*. 2009; 18(4):279–295.
67. Brady AC, Martino MM, Pedraza E, Sukert S, Pileggi A, Ricordi C, Hubbell JA, Stabler CL. Proangiogenic hydrogels within macroporous scaffolds enhance islet engraftment in an extrahepatic site. *Tissue Eng Part A*. 2013; 19(23–24):2544–52. [PubMed: 23790218]
68. Pedraza E, Brady AC, Fraker CA, Stabler CL. Synthesis of macroporous poly (dimethylsiloxane) scaffolds for tissue engineering applications. *Journal of Biomaterials Science, Polymer Edition*. 2013; 24(9):1041–1056. [PubMed: 23683037]
69. Salvay D, Rives C, Zhang X, Chen F, Kaufman DB, Lowe WL Jr, Shea LD. Extracellular matrix protein-coated scaffolds promote the reversal of diabetes after extrahepatic islet transplantation. *Transplantation*. 2008; 85(10):1456–1464. [PubMed: 18497687]
70. Gibly RF, Zhang X, Graham ML, Hering BJ, Kaufman DB, Lowe WL, Shea LD. Extrahepatic islet transplantation with microporous polymer scaffolds in syngeneic mouse and allogeneic porcine models. *Biomaterials*. 2011; 32(36):9677–84. [PubMed: 21959005]

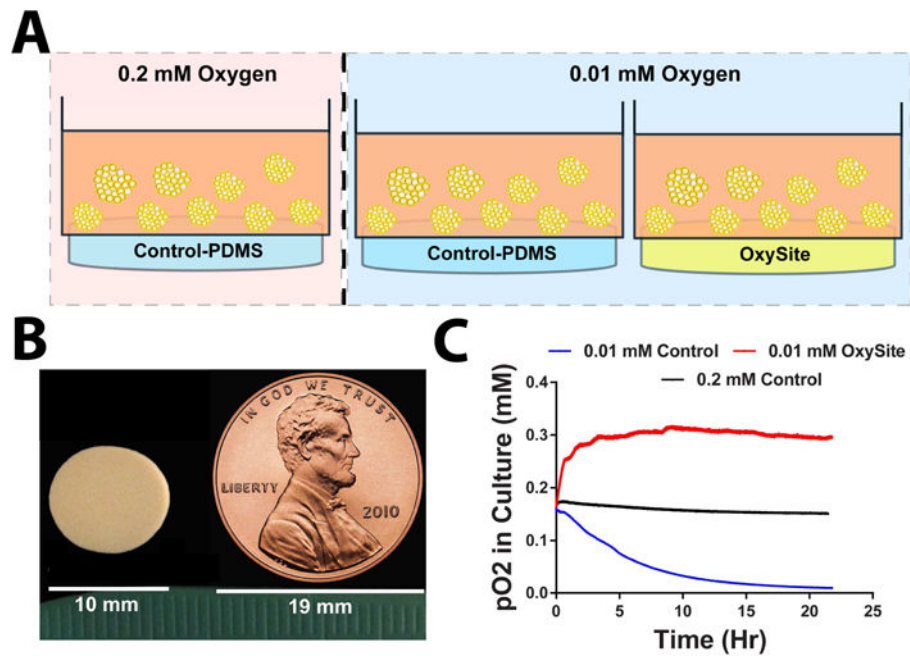


Figure 1. Summary of experimental design and conditions

A) Schematic representation of *in vitro* cultures implemented for experimental assessments, with islets placed within transwells and contro-PDMS or OxySite disks placed underneath.

B) Photograph of OxySite disk, with US penny as scale reference.

C) Oxygen trace measurements recorded *in vitro* in cell-free conditions for standard 0.2 mM culture (black line); low 0.01 mM oxygen (blue line); and low oxygen (0.01 mM) plus Oxysite (red line) conditions.

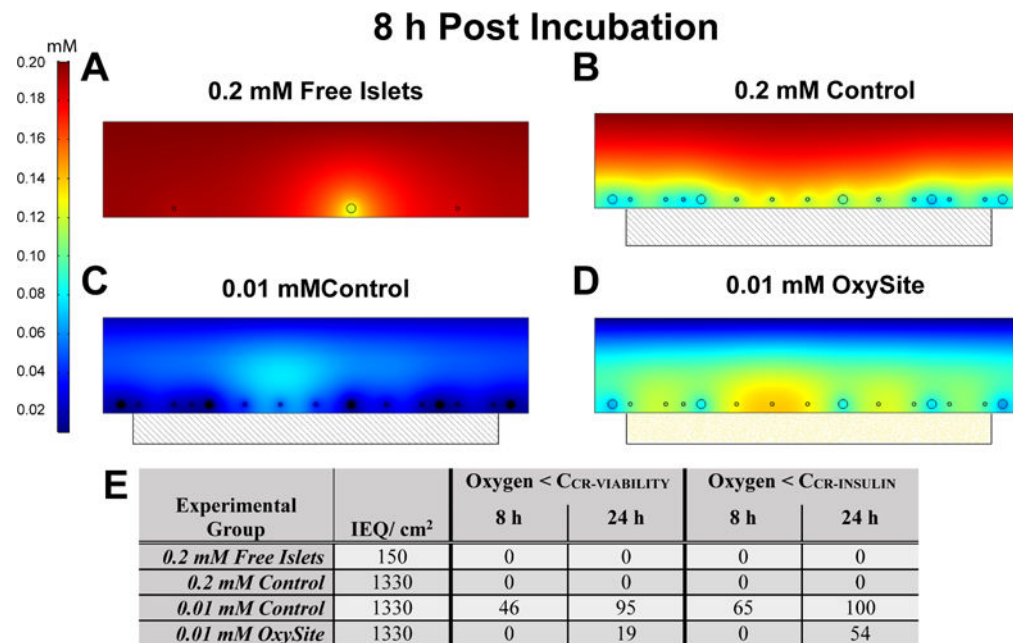


Figure 2. Representative FEM simulation models illustrating effects of loading densities and external oxygen tensions on oxygen availability to pancreatic islets after 8 h of culture Culture conditions varied from A) standard oxygen and loading density (*Free Islets*); B) standard oxygen and high loading density with a PDMS blank control (*0.2 mM Oxygen Control*); C) low oxygen and high density with a PDMS blank control (*0.01 mM Oxygen Control*); or D) low oxygen and high density with an OxySite disk (*0.01 mM OxySite*). Hypoxic areas were defined as zones with an oxygen concentration below 1×10^{-4} mol/m³ and labeled black. Scale = mM oxygen E) Summary of predicted oxygen impacts on cultured islets. % area of total islet area (cross-section) where the oxygen tension was below necrotic (C_{CR-VIABILITY}) or non-functional (CCR-INSULIN) levels, as predicted from multiphysics modeling.

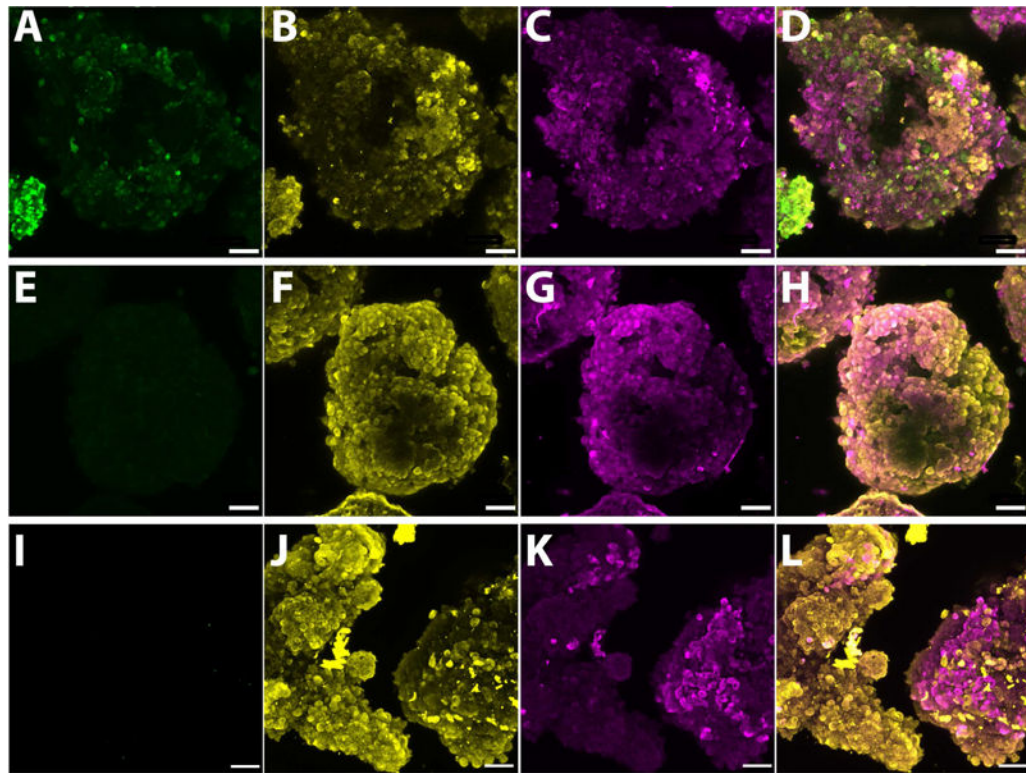


Figure 3. OxySite mitigates accumulation of oxygen-sensitive dyes within rat islets cultured under low oxygen tension

Confocal microscopy whole-mount images of rat islets after 24 h culture under low oxygen (0.01 mM) without (A–D), with OxySite (E–H) or under standard oxygen (0.2 mM, I–L). Islets were stained with oxygen sensitive hypoxyprom (green, A, E & I), insulin (yellow, B, F & J), and glucagon (magenta, C, G & K). Composite image of all stains (D, H & L). Scale bar = 50 μm .

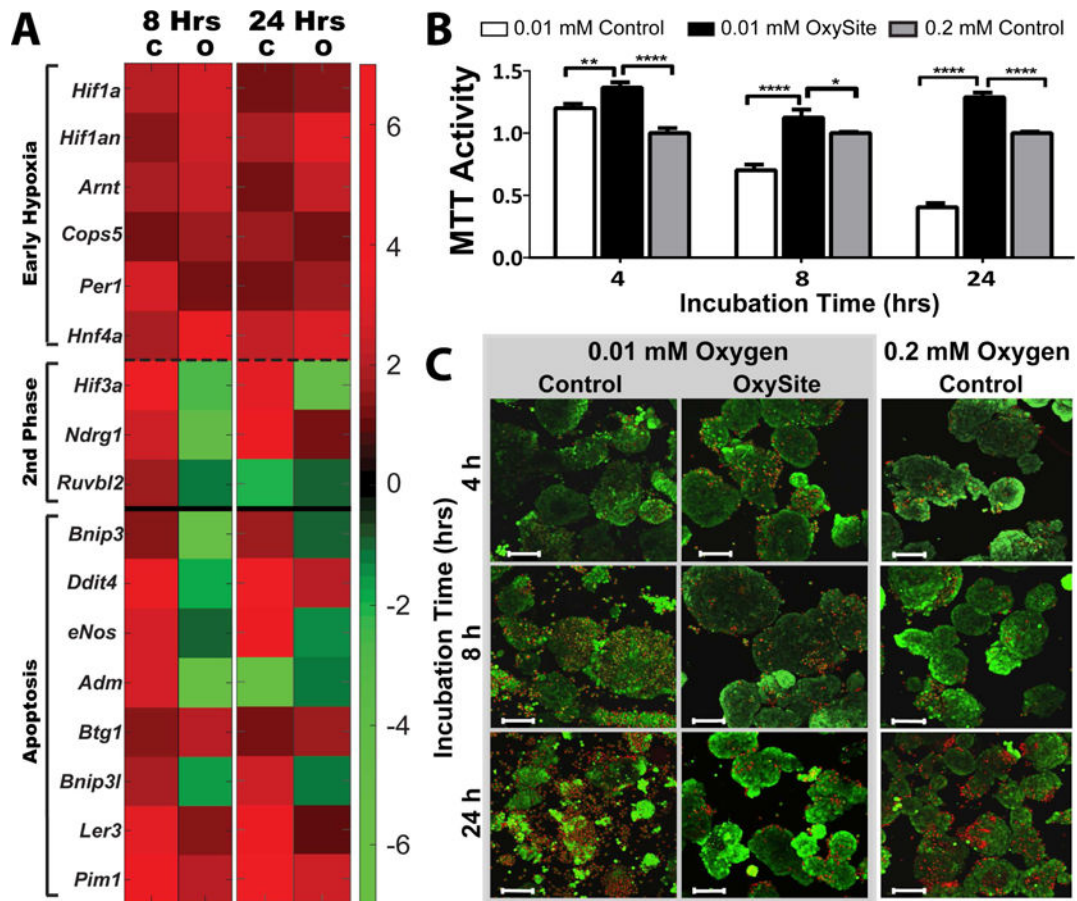


Figure 4. OxySite mitigates activation of second stage hypoxic and apoptotic markers, leading to preservation of metabolic activity and viability

A) Heatmap summary of differential gene expression of early (above dashed line) and second stage (below dashed line) stage hypoxic and apoptotic (below solid line) markers from islets following low oxygen (0.01 mM) culture without (C) or with OxySite (O) after 8 and 24 h. Results are expressed as fold regulation over standard oxygen (0.2 mM) controls, with increased (red) or decreased (green) fold expression scaled according to scale bar shown. **B)** Metabolic activity (measured via MTT) for islets following 4, 8, and 24 h culture under low oxygen (0.01 mM) without (white bars) or with OxySite (black bars), compared to standard oxygen (0.02 mM) controls (grey bars). * p < 0.05, ** p < 0.01, **** p < 0.0001. **C)** Visualization of islet viability via live/dead staining (green = live; red = dead) after 4, 8, and 24 hr culture under 0.01 mM oxygen without (Control; left panel) or with OxySite (middle panel), compared to 0.2mM Oxygen control cultures (right panel). Scale bar = 100 μm.

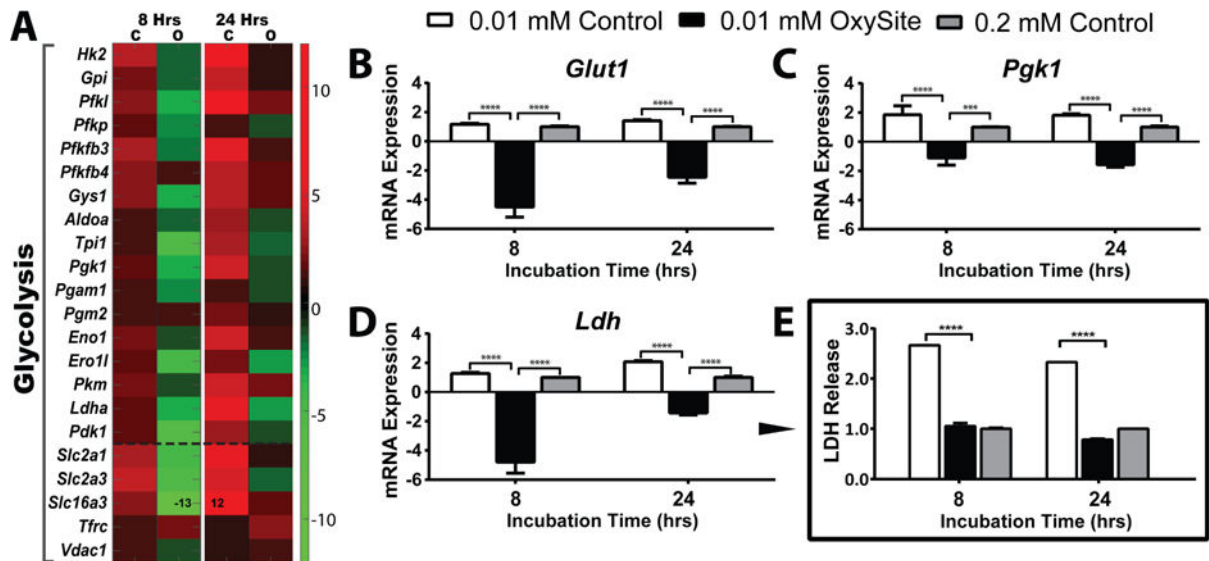


Figure 5. OxySite mitigates activation of anaerobic glycolysis for rat pancreatic islets cultured under hypoxic conditions

A) Heatmap summary of differential gene expression of glycolysis (above dashed line: glycolytic pathway; below dashed line: membrane glucose transporters) from islets following low oxygen (0.01 mM) culture without (C) or with OxySite (O) after 8 and 24 h. Results are expressed as fold regulation over standard oxygen (0.2 mM) controls, with increased (red) or decreased (green) fold expression scaled according to scale bar shown. **B–D)** qRT-PCR of selected glycolytic genes *Glut1*, *Pgk1*, and *Ldh* quantify the extent of anaerobic glycolytic gene activation in low oxygen (0.01 mM) control (white bars) islets after 8 and 24 h culture, compared to 0.01 mM oxygen OxySite treated (black bars) and 0.02 mM oxygen control (grey bars) islets. **E)** Protein levels of LDH following hypoxic exposure for all culture groups. *** $p < 0.0005$, **** $p < 0.0001$.

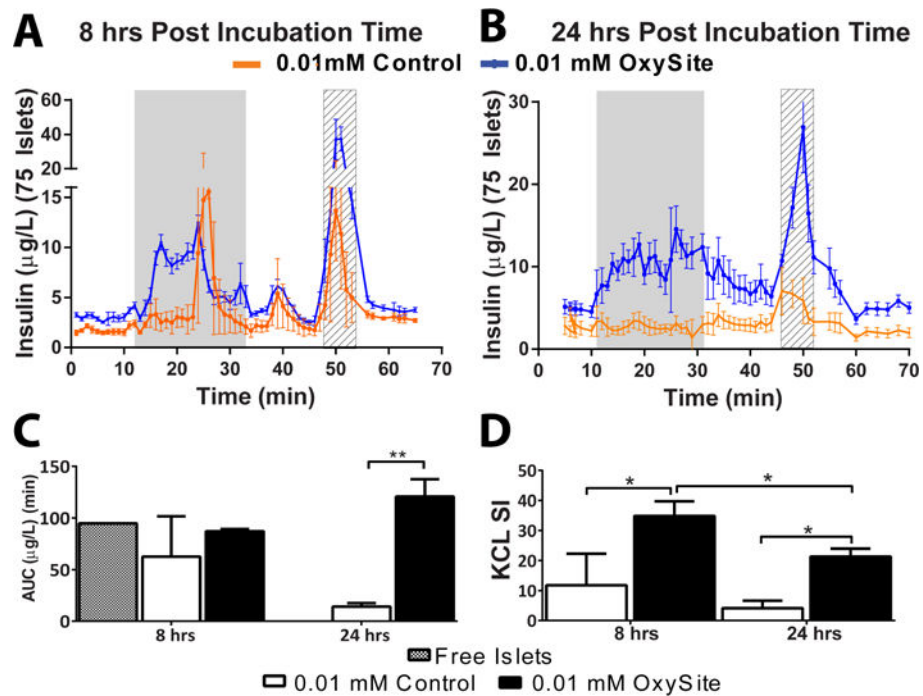


Figure 6. OxySite preserves glucose stimulated insulin release for rat pancreatic islets cultured under hypoxic conditions

A–B) Dynamic glucose perfusion and resulting insulin release from islets cultured under low oxygen (0.01 mM) without (orange) or with OxySite (blue) after acute (8 h; **A**) and chronic (24 h; **B**) culture. Grey region = high glucose (11 mM); Striped region = KCl **C**) Resulting area under the curve (AUC) of insulin release during high glucose stimulation for low oxygen cultures without (white bar) or with OxySite (black bar), compared to islet cultured under standard oxygen and density conditions (free islets; grey bar). **D**) KCL Stimulation Index (SI) for low oxygen cultures without (white bar) or with OxySite (black bar). * $p < 0.05$, ** $p < 0.01$.

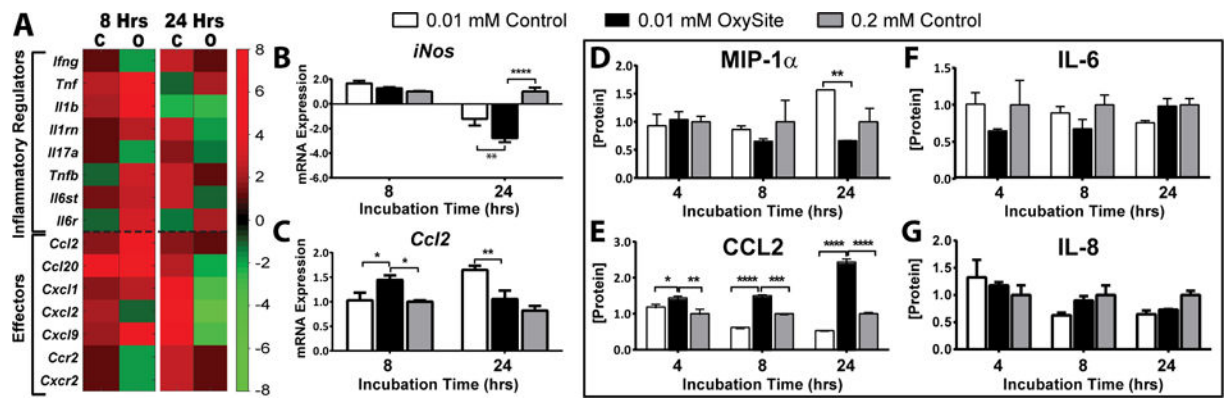


Figure 7. OxySite alters expression of inflammatory regulators and effectors of rat pancreatic islets under hypoxic conditions

A) Heatmap summary of differential gene expression of inflammatory regulators (above dashed line) and effectors (below dashed line) from islets following low oxygen (0.01 mM) culture without (C) or with OxySite (O) after 8 and 24 h. Results are expressed as fold regulation over standard oxygen (0.2 mM) controls, with increased (red) or decreased (green) fold expression scaled according to scale bar shown. **B–C)** qRT-PCR of selected inflammatory genes (*iNos* and *Ccl2*) quantify the extent of cytokine gene expression activation in low oxygen (0.01 mM) control (white bars) islets after 8 and 24 h culture, compared to 0.01 mM oxygen OxySite treated (black bars) and 0.02 mM oxygen control (grey bars) islets. **D–G)** Protein levels of cytokines MIP1 α , CCL2, IL-6, and IL-8 in the culture supernatant after 8 and 24 h incubation under low oxygen conditions without (white bars) or with OxySite (black bar), compared to 0.2 mM control cultures (grey bars). * $p < 0.05$, ** $p < 0.01$, *** $p < 0.0005$, **** $p < 0.0001$.

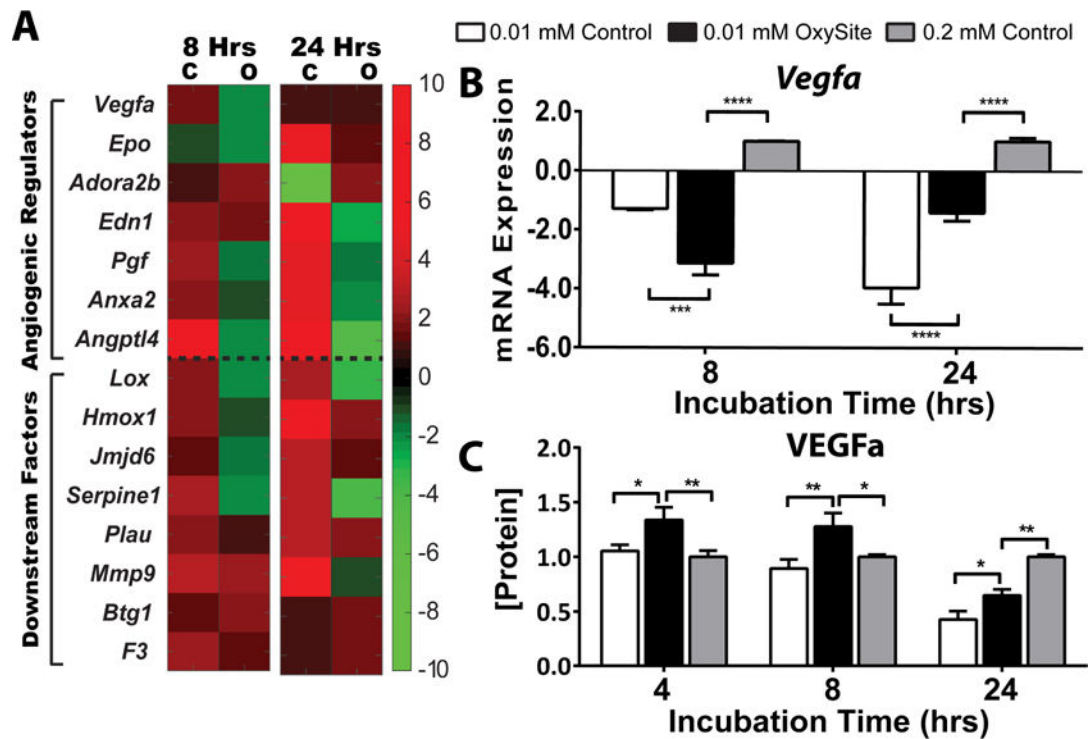


Figure 8. Impact of OxySite on angiogenic pathways and VEGF protein release for low oxygen cultures of rat islets

A) Heatmap summary of differential gene expression of angiogenic gene regulators (above dashed line) and downstream factors (below dashed line) from islets following low oxygen (0.01 mM) culture without (C) or with OxySite (O) after 8 and 24 h. Results are expressed as fold regulation over standard oxygen (0.2 mM) controls, with increased (red) or decreased (green) fold expression scaled according to scale bar shown. **B)** qRT-PCR of *Vegfa* quantifies the extent of gene expression activation in low oxygen (0.01 mM) control (white bars) islets after 8 and 24 h culture, compared to 0.01 mM oxygen OxySite treated (black bars) and 0.02 mM oxygen control (grey bars) islets. **C)** Protein levels of VEGFa in culture media after 8 and 24 h culture under low oxygen conditions without (white bars) or with OxySite (black bar), compared to 0.2 mM control cultures (grey bars). * $p < 0.05$, ** $p < 0.01$, *** $p < 0.0005$, **** $p < 0.0001$.

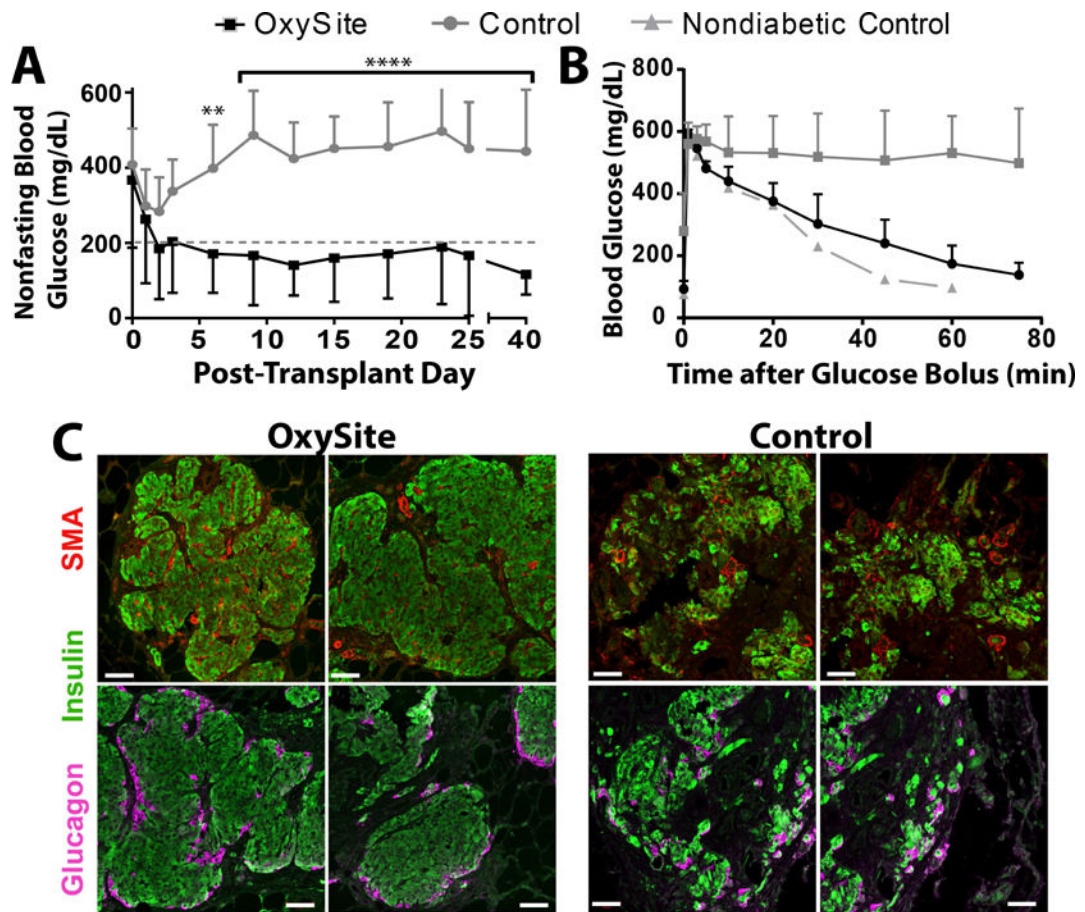


Figure 9. Co-culture of rat islets with OxySite resulted in enhanced functional outcomes when transplanted into diabetic syngeneic recipients

A) Average nonfasting blood glucose levels of rats receiving islets cultured under low oxygen (0.01 mM) conditions with OxySite for 24 h prior to transplant (black squares; $n = 8$). Control islets were cultured under standard oxygen (0.2 mM) for 24 h prior to transplant (grey circles; $n = 8$) or with a blank PDMS (grey line; $n=8$). **B)** Tracking of glucose clearance following intravenous glucose tolerance test (IVTT) performed in a subset of animals at 30 d post-transplant. Metabolic clearance was compared to a nondiabetic rat. (OxySite $n = 5$; Control, $n = 3$; Nondiabetic control, $n = 1$). **D)** Immunohistochemistry evaluation of grafts explanted 40 days post-transplant, stained with anti-insulin (green), anti-smooth muscle actin (SMA, red), and nuclear staining (blue) (top row) or anti-insulin (green), anti-glucagon (pink), and nuclear staining (blue) (top row). Scale bar = 50 μm .